

Collective versus hub activation of epidemic phases on networks

Silvio C. Ferreira,^{1,*} Renan S. Sander,¹ and Romualdo Pastor-Satorras²

¹*Departamento de Física, Universidade Federal de Viçosa, 36570-000, Viçosa, MG, Brazil*

²*Departament de Física, Universitat Politècnica de Catalunya, Campus Nord B4, 08034 Barcelona, Spain*

We consider a general criterion to discern the nature of the threshold in epidemic models on scale-free (SF) networks. Comparing the epidemic lifespan of the nodes with largest degrees with the infection time between them, we propose a general dual scenario, in which the epidemic transition is either ruled by a hub activation process, leading to a null threshold in the thermodynamic limit, or given by a collective activation process, corresponding to a standard phase transition with a finite threshold. We validate the proposed criterion applying it to different epidemic models, with waning immunity or heterogeneous infection rates in both synthetic and real SF networks. In particular, a waning immunity, irrespective of its strength, leads to collective activation with finite threshold in scale-free networks with large exponent, at odds with canonical theoretical approaches.

PACS numbers: 05.40.Fb, 89.75.Hc, 89.75.-k

I. INTRODUCTION

The study of epidemic spreading [1] in complex topologies is one of the cornerstones of modern network science [2], with applications in the spread of influence, opinions and other social phenomena [3, 4]. Of particular interest is the theoretical understanding of epidemic models in scale-free (SF) networks [5], in which the probability $P(k)$ (degree distribution) that a node is connected to k others (has degree k) exhibits heavy tails of the form $P(k) \sim k^{-\gamma}$. This interest is motivated by the possible effects that a heterogeneous topology might have on the location of the epidemic threshold λ_c , for some control parameter λ , signaling a phase transition separating a healthy, disease-free phase, from an infected phase, in which the epidemics can thrive [1].

For epidemics leading to a steady (endemic) state, the main object of interest has been the susceptible-infected-susceptible (SIS) model, which is defined as follows [6]: Individuals, represented as nodes in the network, can assume two different states, susceptible (S) or healthy, and infected (I), and are capable to transmit the disease. Infected individuals recover and become spontaneously susceptible again with a rate β that can be taken equal to 1. Transmission of the disease is effected by a rate to transmit the disease through an edge connecting an infected to a susceptible node equal to a constant λ . After a considerable theoretical effort, it has been shown that the behavior of the SIS model in uncorrelated [2] SF networks is far from trivial [7–16]. Two competing theories were initially proposed to account for the SIS epidemic threshold. Heterogeneous mean-field (HMF) theories [1], neglecting both dynamical and topological correlations, provide a threshold $\lambda_c^{\text{HMF}} = \langle k \rangle / \langle k^2 \rangle$ [8, 17], which tends to zero in the thermodynamic limit for $\gamma \leq 3$, and is finite for $\gamma > 3$. Quenched mean-field (QMF) theory [9], including the full network structure through its adjacency matrix A_{ij} [2],

but still neglecting dynamical correlations, predicts instead a threshold $\lambda_c^{\text{QMF}} \simeq 1/\Lambda_m$, where Λ_m is the largest eigenvalue of the adjacency matrix. The scaling form of this threshold is given by [11, 18] $\lambda_c^{\text{QMF}} \simeq 1/\sqrt{k_{\text{max}}}$ for $\gamma > 5/2$, where k_{max} is the maximum degree in the network, while for $\gamma < 5/2$ it yields $\lambda_c^{\text{QMF}} \simeq \langle k \rangle / \langle k^2 \rangle$ in agreement with HMF theory. Numerical simulations [11, 12, 14] indicate that QMF is qualitatively correct in SF networks, implying that the epidemic threshold vanishes in the thermodynamic limit when k_{max} diverges, irrespective of the degree exponent γ .

The origin of this null threshold has been physically interpreted in Ref. [14] taking explicitly into account the interplay between the lifetime of a hub of degree k , τ_k^{rec} , and the time scale $\tau_{k,k'}^{\text{inf}}$ with which an infected hub of degree k infects a susceptible hub of degree k' . The fact that the lifetime τ_k^{rec} is diverging with degree k faster than $\tau_{k,k'}^{\text{inf}}$ for any value of λ is the ultimate cause of the null epidemic threshold in the SIS model [10, 14, 15]. However, other epidemic and dynamical models on SF networks, in particular the contact process (CP)[19], defined by an infection rate inversely proportional to the degree of the infected node, λ/k , possess a finite threshold which can be better captured in terms of a degree-based HMF theory [20, 21]. This observation claims for an understanding of the mechanisms ruling epidemic transitions, regarding in particular the conditions under which the threshold is either constant or vanishing.

The results of Ref. [14], while important, are strictly applied to the SIS process, and thus a general formalism, adapted to more complex and realistic epidemic models with a steady state, is still lacking. Here we determine the recovery τ^{rec} and infection τ^{inf} time scales of hubs for generic epidemic models including waning immunity and arbitrary edge-dependent infection rates and, building on these results, we propose a classification of endemic epidemic transitions on networks: When $\tau^{\text{rec}} \gg \tau^{\text{inf}}$, a scenario of local hub activation with mutual hub re-infection is at work [14], leading to $\lambda_c \rightarrow 0$ when the recovery times diverges in the thermodynamic limit. In such scenario, QMF theories are expected to be qualita-

* silviojr@ufv.br

tively correct. On the other hand, for $\tau^{\text{rec}} \leq \tau^{\text{inf}}$, mutual hub reinfection cannot take place, and an endemic state is possible only through a collective activation of the whole network in a standard phase transition occurring at a finite threshold. In this second scenario, HMF theories should be correct.

We present evidence for this scenario analyzing the susceptible-infected-removed-susceptible (SIRS) model [6], an extension of the SIS model allowing for a waning immunity of nodes. While it has been shown that SIRS is equivalent to SIS dynamics in the framework of standard mean-field theories [22], here we show that the effect of waning immunity is to induce a finite threshold in SF networks for $\gamma > 3$, at odds with QMF and qualitatively described by HMF theory. For sake of generality, the theory is also applied to other epidemic models without immunity, namely, the CP [19] and the generalized SIS model proposed by Karsai, Juhász, and Iglói (KJI) [23] with weighted infection rates.

Our paper is organized as follows: We develop the theory for the interplay between of hub lifetime and mutual hub infection time in Section II and corroborate the theory with simulations on synthetic and real SF networks in sections III and IV, respectively. We briefly summarize our conclusions and prospects in section V. Three appendices complement the paper: HMF and QMF theories for investigated models are presented in appendices A and B while simulation methods are presented in appendix C.

II. THEORY

A. The generalized epidemic model

To develop our theory we study a generalized epidemic model on a network where each vertex can be either healthy or susceptible (S), infected (I), and immune or recovered (R). Infected individuals recover spontaneously, $I \rightarrow R$, with rate β . Recovered individuals become again spontaneously susceptible (waning immunity) $R \rightarrow S$, with a rate α . Infected nodes of degree k transmit the disease to each adjacent susceptible node of degree k' with an heterogeneous infection rate $\lambda_{k,k'}$. See Figs. 1(a) and 1(b) for a graphical description of the model. From this generalized epidemic model, classical ones can be recovered: The SIS model ($\alpha \rightarrow \infty$, $\lambda_{k,k'} = \lambda$); the CP [19] model ($\alpha \rightarrow \infty$, $\lambda_{k,k'} = \lambda/k$); the SIRS model (α finite, $\lambda_{k,k'} = \lambda$); the KJI [23] model ($\alpha \rightarrow \infty$, $\lambda_{k,k'} = \lambda/(kk')^\theta$), etc.

To be used later, we define the average infection rate produced, λ_k^{out} , and received, λ_k^{in} , by a vertex of degree k as

$$\lambda_k^{\text{out}} = \sum_{k'} \lambda_{kk'} P(k'|k), \quad \lambda_k^{\text{in}} = \sum_{k'} \lambda_{k'k} P(k'|k), \quad (1)$$

respectively, where $P(k'|k)$ is the probability that a vertex of degree k is connected to vertex of degree k' [24].

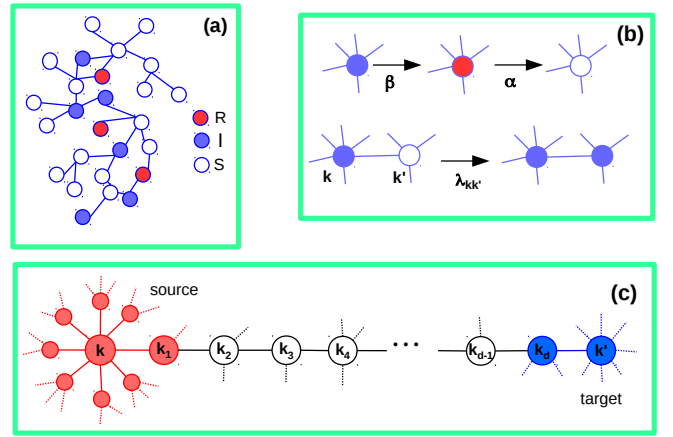


Figure 1. (color online) Generic epidemic model in complex networks. (a) Nodes in the network can be either healthy or susceptible (S), infected (I), and immune or recovered (R). (b) Infected individuals recover spontaneously, $I \rightarrow R$, with rate β . Recovered individuals become again spontaneously susceptible, $R \rightarrow S$, with a rate α . Heterogeneous transmission is implemented by infected nodes of degree k transmitting the disease to adjacent susceptible nodes of degree k' with rate $\lambda_{k,k'}$. (c) Schematic representation of chain of d vertices of arbitrary degrees k_1, k_2, \dots, k_d , connecting two hubs of degree k and k' . The infection starting in the center of the leftmost star (red) aims to reach the rightmost star (blue). Stubs as dashed lines represent edges that can transmit but cannot receive the infection.

B. Hub lifetime

We focus in the first place on the hub lifetime τ_k^{rec} , which is defined as the average time that a hub of degree k , starting from a configuration with a single infected node, takes to reach a configuration in which the hub and its nearest neighbors are all susceptible. To estimate this quantity, we approximate the dynamics of a hub of degree k by that of a star-like graph, composed by a center connected to k nodes (leaves) of arbitrary degree, the red nodes in Fig. 1(c), where we neglect infection coming from outside the star. For analytical tractability, we consider a simplified generic epidemic process with two states (S, I) in the leaves and three states (S, I, R) in the center. The rate of infection along an edge from a leaf to the center is approximated by λ_k^{in} and from the center to a leaf by λ_k^{out} , see Eq. (1); that is, we consider the effect of the leaves as an average over their possible degree values k' , weighted with the probability $P(k'|k)$. The transitions $I \rightarrow S$ (leaves), $I \rightarrow R$ and $R \rightarrow S$ (center) have constant rates β , β , and α , respectively. The lifespan for this dynamics is larger than in the real model, where leaves can also assume the R state, and so it provides an upper bound for the true τ_k^{rec} .

We approximate this dynamics in a star as follows:

i) At $t = 0$ the center is infected and all leaves are susceptible.

ii) At time $t_1 = 1/\beta$ the center becomes recovered and

n_1 leaves are infected with probability

$$P_1(n_1|k) = \binom{k}{n_1} p_1^{n_1} (1-p_1)^{k-n_1}, \quad (2)$$

where $p_1 = 1 - \exp(-\lambda_k^{\text{out}}/\beta)$ is the probability that each leaf was infected by the center in the interval $t < t_1$.

iii) At time $t = t_1 + t_2$, where t_2 has a distribution $\rho_2(t_2) = \alpha \exp(-\alpha t_2)$, the center becomes susceptible and n_2 leaves remain infected with probability

$$P_2(n_2|n_1) = \binom{n_1}{n_2} p_2^{n_2} (1-p_2)^{n_1-n_2}, \quad (3)$$

where $p_2 = \exp(-\beta t_2)$ is the probability that each active leaf remains infected for a time t_2 .

iv) At time $t = t_1 + t_2 + t_3$, where $t_3 = 1/\beta$, all n_2 leaves infected at time $t_1 + t_2$ become (synchronously) susceptible and the center is infected again with probability

$$P_3(n_2) = 1 - (1-p_3)^{n_2}, \quad (4)$$

where $p_3 = 1 - \exp(-\lambda_k^{\text{in}}/\beta)$ is the probability that each leaf sent the infection to the center during a time t_3 .

Steps ii) and iv) are essentially a generalization of the approximation for SIS dynamics on stars in Ref. [14], in which stochasticity of infective time and multiple infections of the leaves are neglected, while step ii) does not involve approximations. Treating step ii) stochastically is essential since the rare events in which only a few infected leaves survive cannot be neglected. The probability that the star returns to its initial state in one step with interevent times t_1 , t_2 and t_3 is

$$q_k(t_2) = \sum_{n_1=1}^k P_1(n_1|k) \sum_{n_2=1}^{n_1} P_2(n_2|n_1) P_3(n_2) \quad (5)$$

Averaging $q_k(t_2)$ over $\rho_2(t_2)$ we finally have

$$Q_k = 1 - \alpha \int_0^\infty e^{-\alpha t_2} [1 - e^{-\beta t_2} A]^k dt_2, \quad (6)$$

with $A = (1 - e^{-\lambda_k^{\text{out}}/\beta})(1 - e^{-\lambda_k^{\text{in}}/\beta})$. Now, the probability that this dynamics survives for s steps of average duration $\tau_0 = t_1 + \langle t_2 \rangle + t_3 = 2/\beta + 1/\alpha$ is $P(s) = Q_k^{s-1}(1 - Q_k)$ and the average number of survival steps is $\langle s \rangle = \sum_{s=1}^\infty s P(s) = 1/(1 - Q_k)$. We thus obtain the final result

$$\tau_k^{\text{rec}} \equiv \tau_0 \langle s \rangle = \frac{\tau_0}{1 - Q_k}. \quad (7)$$

Considering the absence of waning immunity inserting in Eq. (6) the limit $\lim_{\alpha \rightarrow \infty} \alpha e^{-\alpha t} = \delta(t)$, the Dirac delta function, and assuming $\lambda_k^{\text{in}}/\beta, \lambda_k^{\text{out}}/\beta \ll 1$, we obtain

$$\tau_k^{\text{rec}} \sim \exp(k \lambda_k^{\text{in}} \lambda_k^{\text{out}} / \beta^2). \quad (8)$$

In the case of α finite, Eq. (6) becomes, after the change of variable $u = A e^{-\beta t}$,

$$Q_k = 1 - \frac{\alpha}{\beta A^{\alpha/\beta}} \int_0^A u^{\alpha-1} (1-u)^k du. \quad (9)$$

We can estimate the behavior of Q_k in the limit of large k using

$$(1-u)^k = \exp[k \ln(1-u)] \simeq e^{-uk}, \quad (10)$$

valid for $0 < u \ll 1$, and

$$\int_0^A u^{\alpha-1} e^{-uk} du \simeq \int_0^\infty u^{\alpha-1} e^{-uk} du = k^{-\alpha} \Gamma(\alpha), \quad (11)$$

where $\Gamma(z)$ is the gamma function [25], and in which the extension of the integral's upper limit to infinity is valid for kA large. Thus, from Eq. (9), we obtain

$$Q_k \simeq 1 - \frac{\alpha}{\beta A^{\alpha/\beta}} \Gamma\left(\frac{\alpha}{\beta}\right) k^{-\alpha/\beta}. \quad (12)$$

From here and Eq. (7), it follows in the limit of large k

$$\tau_k^{\text{rec}} \sim k^{\alpha/\beta} \left[(1 - e^{-\lambda_k^{\text{out}}/\beta})(1 - e^{-\lambda_k^{\text{in}}/\beta}) \right]^{\alpha/\beta}. \quad (13)$$

C. Hub mutual infection time

To estimate the infection time $\tau_{k,k'}^{\text{inf}}$, we consider two stars of degree k (the source $i = 0$) and k' (the target at $i = d + 1$), connected through a path of d vertices ($i = 1, 2, \dots, d$) of arbitrary degree, see Fig. 1. The following hypothesis are used in the derivation for the case $\tau_k^{\text{rec}} \gg 1/\lambda_k^{\text{out}}$:

i) The vertex with degree k on the left ($i = 0$) is never recovered and transmits the infection to its nearest neighbor at $i = 1$ at an average rate λ_k^{out} and, in an average, a new epidemic outbreak is started at $i = 1$ each $1/\lambda_k^{\text{out}}$ time units.

ii) We assume that both $\lambda_{kk'}/\beta \ll 1$ and $\lambda_{kk'}/\alpha \ll 1$ and consider only the epidemic routes where an infected vertex always transmit the infection to its right neighbor before it becomes recovered or susceptible [14]. Additionally, we assume the average transmission rate for all edges inside the chain ($i = 1, \dots, d-1$) $\bar{\lambda} = \sum_{k'} \lambda_k^{\text{out}} P(k)$ that leads to the average probability of transmission per edge given by $\bar{q} = \bar{\lambda}/(\bar{\lambda} + \beta)$.

iii) The rate at which an infected vertex at $i = d$ transmits the infection to the rightmost hub of degree k' at $i = d + 1$ is approximated by $\lambda_{k'}^{\text{in}}$. The average probability to transmit do $i = d + 1$ before recovering of $i = d$ is, therefore, $\bar{q}_{k'} = \lambda_{k'}^{\text{in}}/(\lambda_{k'}^{\text{in}} + \beta)$.

iv) The probability that an infection started at $i = 1$ reaches the rightmost hub ($i = d + 1$) under these assumptions is given by $\bar{q}^{d-2} \bar{q}_{k'}$ and, consequently, the transmission rate is $\lambda_k^{\text{out}} \bar{q}^{d-2} \bar{q}_{k'}$.

v) For small-world networks with N vertices, the average distance between nodes of degrees k and k' is [26]

$$d = 1 + \ln(N \langle k \rangle / k k') / \ln \kappa, \quad (14)$$

where $\kappa = \langle k^2 \rangle / \langle k \rangle - 1$, resulting in an upper bound for the infection time (inverse of the rate) given by

$$\tau_{k,k'}^{\text{inf}} \lesssim \tau_{kk'} = \frac{\bar{q}_{k'}}{\lambda_k^{\text{out}} \bar{q}} \left(\frac{N \langle k \rangle}{k k'} \right)^{b(\bar{\lambda})}, \quad (15)$$

where $b(\bar{\lambda}) = \ln(1 + \beta/\bar{\lambda})/\ln \kappa$.

For the case $\tau_k^{\text{rec}} < 1/\lambda_k^{\text{out}}$, the leftmost star recovers before produce the first outbreak in $i = 1$ and thus the infection time becomes infinite.

III. ANALYSIS OF EPIDEMIC MODELS ON SYNTHETIC SCALE-FREE NETWORKS

In this Section we present the analysis of different epidemic models on SF networks characterized by a degree distribution $P(k) \sim k^{-\gamma}$, that in a network of finite size N extends up to a maximum degree [27]

$$k_{\text{max}}(N) \sim \begin{cases} N^{1/2} & \text{for } \gamma < 3 \\ N^{1/(\gamma-1)} & \text{for } \gamma > 3 \end{cases}. \quad (16)$$

In these networks, we have

$$\kappa \sim \begin{cases} k_{\text{max}}^{3-\gamma} \simeq N^{(3-\gamma)/2} & \text{for } \gamma < 3 \\ \text{const.} & \text{for } \gamma > 3 \end{cases} \quad (17)$$

We focus in particular in uncorrelated networks, with $P(k'|k) = k'P(k')/\langle k \rangle$ [28], as generated by the uncorrelated configuration (UCM) model [29].

A. SIS model

The SIS model is defined by $\alpha = 0$ and $\lambda_{k,k'} = \lambda$, independent of k and k' , yielding $\lambda_k^{\text{in}} = \lambda_k^{\text{out}} = \lambda$. This values imply, from Eq. (8), $\tau_k^{\text{rec,SIS}} \sim \exp(\lambda^2 k/\beta)$. On the other hand, from Eq. (15), and using Eq. (17), we obtain a $\tau_k^{\text{inf,SIS}}$ that is constant for $\gamma < 3$ ($b \rightarrow 0$), while for $\gamma > 3$ ($b \rightarrow \text{const}$) it shows an algebraic increase, that, for the largest hubs with degree k_{max} given by Eq. (16) takes the form $\tau_k^{\text{inf,SIS}} \sim N^{\frac{\gamma-3}{\gamma-1}b(\lambda)}$. Both expressions have been confirmed by means of numerical simulations of the SIS model in Ref. [14]. We have thus that, for the SIS model, $\tau_k^{\text{rec,SIS}} \gg \tau_k^{\text{inf,SIS}}$, i.e. the hubs survive for much longer times than are needed for a hub to reinfect another, and therefore it is plausible a scenario in which the transition is ruled by a hub activation dynamics. This possibility is substantiated by an analysis of the SIS dynamics within a theory taking into account, at a mean-field level, the dynamics of hub recovery and mutual reinfection, leading to a vanishing epidemic threshold scaling with network size in qualitative agreement with the predictions of QMF theory [14]

B. Contact process

In the case of the CP [19], we have $\alpha = \infty$ and $\lambda_{k,k'} = \lambda/k$ implying $\lambda_k^{\text{in}} = \lambda/\langle k \rangle$ and $\lambda_k^{\text{out}} = \lambda/k$, and thus, from Eq. (8), $\tau_k^{\text{rec,CP}} \sim \text{const}$. On the other hand, $1/\lambda_k^{\text{out}}$, and thus $\tau_k^{\text{inf,CP}}$, diverges implying that, for any value of γ , $\tau_k^{\text{rec,CP}} \ll \tau_k^{\text{inf,CP}}$. This result indicates that

it is impossible to have a scenario in which the transition is driven by the successive activation and reactivation of hubs, and that the associated epidemic transition must be given by collective phenomenon, involving the activation of the whole network. This collective transition is consistent with the finite threshold numerically observed in the CP on SF networks [20, 21], in agreement with HMF predictions [19, 21]. Interestingly in the case of the CP, the QMF prediction [30] coincides with the HMF theory [19], $\lambda_c = 1$, indicating a threshold completely independent of the network structure. This theoretical prediction it is not fully observed in numerical simulations, which show a constant threshold but that is modulated by network heterogeneity [19–21]

C. KJI model

The KJI model is defined by $\alpha \rightarrow \infty$ and a heterogeneous infection rate $\lambda_{k,k'} = \lambda/(kk')^\theta$, with $0 \leq \theta \leq 1$; that is, the infection power decreases with the degree of both the infected and susceptible nodes connected by the corresponding edge.

Simple HMF theory [23] (see Appendix A) predicts a threshold in uncorrelated networks

$$\lambda_c^{\text{HMF,KJI}} = \frac{\langle k \rangle}{\langle k^2(1-\theta) \rangle}, \quad (18)$$

which takes a finite value for $\gamma > 3 - 2\theta$, and in particular for $\gamma > 3$ and any $\theta > 0$. On the other hand, QMF theory (see Appendix A) predicts

$$\lambda_c^{\text{QMF,KJI}} = \frac{1}{\Lambda_m^D}, \quad (19)$$

where Λ_m^D is the largest eigenvalue of the matrix $D_{ij} = A_{ij}/(k_i k_j)^\theta$, A_{ij} being the adjacency matrix. This largest eigenvalue (see Appendix A) increases with network size for $\theta < 1/2$ irrespective of γ . Therefore the QMF prediction is a vanishing threshold for $\theta < 1/2$, and a finite one otherwise.

Applying Eq. (1) to the present model leads to $\lambda_k^{\text{in}} = \lambda_k^{\text{out}} = \lambda \langle k^{1-\theta} \rangle / (\langle k \rangle k^\theta)$, which translates, from Eq. (8), to a hub recovery time $\tau_k^{\text{rec,KJI}} \sim \exp(\text{const} \cdot k^{1-2\theta})$ that is finite for $\theta > 1/2$ and diverges as a stretched exponential for $\theta < 1/2$. These results are backed up by numerical simulations of the KJI model on star graphs, see Fig. 2.

The mutual infection time of hubs for $\theta < 1/2$ scales similarly as in the SIS dynamics $\tau_k^{\text{inf,KJI}} \sim N^{\frac{\gamma-3}{\gamma-1}b(\lambda)}$ for $\gamma > 3$ and $\tau_k^{\text{inf,KJI}} \sim \text{const}$ for $\gamma < 3$, the only difference being in the factor $\bar{\lambda} = \lambda \langle k^{-\theta} \rangle \langle k^{1-\theta} \rangle / \langle k \rangle$. For $\theta \geq 1/2$, we have $1/\lambda_k^{\text{out}}$ and thus $\tau_k^{\text{inf,KJI}}$ diverging as in the CP case. Thus, in the case $\gamma > 3$, where HMF and QMF predictions disagree markedly for $\theta < 1/2$, we obtain that, for $\theta < 1/2$, the transition should be driven by a hub activation mechanism, since in this region $\tau_k^{\text{rec}} \gg \tau_k^{\text{inf}}$, and thus should correspond to a vanishing threshold, qualitatively in agreement with QMF, which indeed predicts

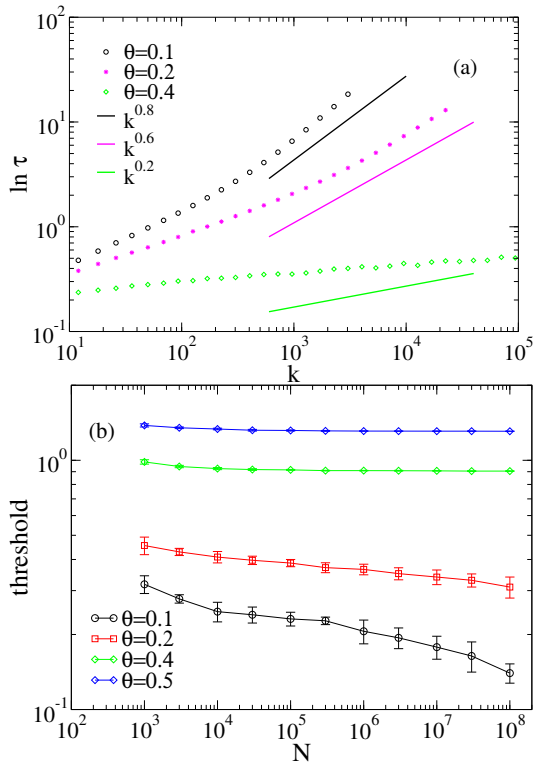


Figure 2. (color online) (a) Lifespan for KJI model on star graphs with $\lambda \langle k^{1-\theta} \rangle / \langle k \rangle = 0.2$ confirming the stretched exponential asymptotic behavior expected for $\theta < 1/2$. (b) Epidemic activation thresholds for the KJI model with different values of θ and $\gamma = 3.5$.

a threshold $\lambda_c^{\text{QMF,KJI}} \sim k_{\text{max}}^{\theta-1/2}$, see Appendix A. For $\theta > 1/2$, on the other hand, the hub lifetime is finite, compatible with a collectively activated transition, and corresponding to a finite threshold, in agreement with both HMF and QMF theories. These predictions are verified in Fig. 2 by means of numerical simulations of the KJI model on SF networks using the quasi-stationary (QS) method [20, 31], estimating the effective threshold for each network size as the position of the main peak shown by the susceptibility $\chi = N(\langle \rho^2 \rangle - \langle \rho \rangle) / \langle \rho \rangle$ (see Appendix C for simulation details). For values of θ close to $1/2$, however, long crossovers are observed in the threshold, in analogy with the behavior observed in the lifespan of stars. Indeed, after a crossover that can be very long as θ approaches $1/2$, the epidemic lifetime of KJI model on star graphs of increasing size reaches the asymptotic regime of a stretched exponential, see Fig. 2. These crossovers, also observed in the numerical estimate of the QMF threshold (see Appendix A), explain the apparently constant threshold observed in Fig 2 for $\theta = 0.4$. Equivalent scenarios can be drawn for $\gamma < 3$ with critical values of θ smaller than $1/2$.

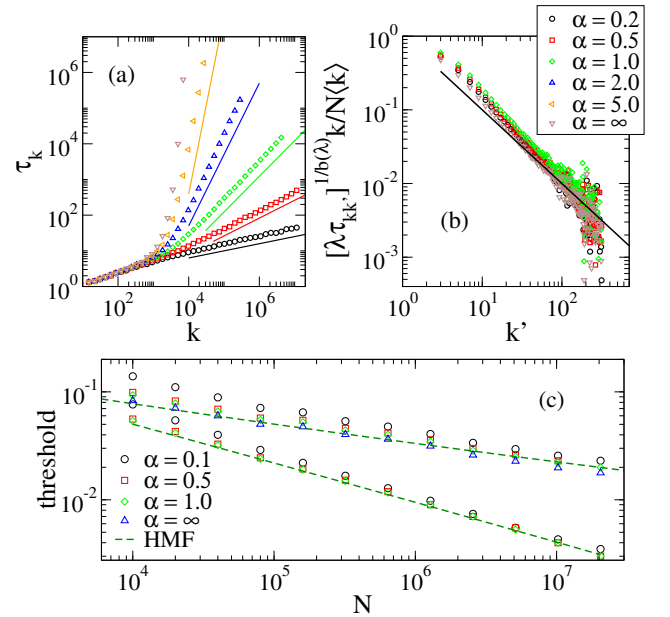


Figure 3. (color online) (a) Lifespan for SIRS/SIS dynamics on star graphs with k leaves for $\lambda = 0.05$, $\beta = 1$ and different values of α . Solid lines are power laws $\tau_k \sim k^{\alpha/\beta}$. (b) Infection times of vertices of degree k' in a network with $N = 10^5$ vertices where the epidemics starts in a vertex of degree $k = 50$ which is never cured. The solid line represents the theoretical value of Eq. (15). (c) Epidemic thresholds against network size for different immunization times $1/\alpha$, using SF networks with degree exponents $\gamma = 2.2$ (bottom curves) and $\gamma = 2.7$ (top curves). Dashed lines correspond to $\lambda_c^{\text{QMF}} = 1/\Lambda_m$, where Λ_m is the largest eigenvalue of the adjacency matrix.

D. SIRS model

We finally consider the SIRS model, an extension of the SIS model, with the same $\lambda_{k,k'}$ constant, but with a finite waning immunity. Application of standard mean field theories (see Appendix B) leads to exactly the same result as the SIS model, independently of the waning immunity α , i.e. $\lambda_c^{\text{HMF,SIRS}} = \langle k \rangle / \langle k^2 \rangle$ and $\lambda_c^{\text{QMF,SIRS}} = 1/\Lambda_m$. So, we face the same situation of the SIS and KJI models, with two contradictory predictions in SF networks for $\gamma > 3$

In the SIS model, from Eq. (13), and given that $\lambda_k^{\text{in}} = \lambda_k^{\text{out}} = \lambda$, we obtain

$$\tau_k^{\text{rec,SIRS}} \sim k^{\alpha/\beta}, \quad (20)$$

that is, an algebraic increase of the hub recovery time with degree, modulated by the exponents α and β . This analytic prediction is confirmed in numerical simulations of the SIRS model using the QS method (see Appendix C for details) in Fig. 3(a). The agreement observed is expected for small λ , since only a few leaves are infected in each step and thus neglecting the recovered leaves at the end of each step becomes a good approximation.

Application of Eq. (15) turns out the same result as in the SIS model, i.e. a finite infection time for $\gamma < 3$

and an algebraic increase for $\gamma > 3$. This result, which is independent of α , is numerically confirmed in Fig. 3(b). At this respect, it is interesting to notice that the basic hypothesis used in our analysis, see Sec. II B, considering only the epidemic routes where the infected vertices always transmit the infection to its right neighbor before it becomes recovered or susceptible [14], is more precise for longer immunization periods (small α) since the multiple infection of a vertex in this path occurs rarely, implying the bound is an estimate of $\tau_{k,k'}^{\text{inf}}$ for SIRS as good as or better than that for SIS.

Combining the previous results, we observe that for $\gamma < 3$, the hub recovery time is always larger than the hub infection time, the same situation observed on the SIS mode, with the only difference of the sharper (exponential) increase of τ_k^{rec} in the SIS case. The scenario that we expect in this range of γ values is thus a SIS-like transition, with the hub reinfection mechanism at work and a vanishing epidemic threshold, in qualitative agreement with QMF. In order to check the prediction, we have performed numerical simulations of the SIRS model on SF networks using the QS method (see Appendix C) for details). In Fig. 3(c) we show that, for $\gamma < 3$, even a very small value of α leads to a scaling of the epidemic threshold against networks sizes in very good agreement with the QMF prediction.

For $\gamma > 3$, on the other hand, the situation is more complex and the threshold finite-size behavior depends on α . From the divergence of the the maximum degree in Eq. (16), we obtain $\tau^{\text{inf,SIRS}} \sim N^{\frac{\gamma-3}{\gamma-1}b(\lambda)}$ and $\tau^{\text{rec,SIRS}} \sim N^{\frac{\alpha/\beta}{\gamma-1}}$, that is, algebraic increases with network size in both cases. A SIS-like regime (hub reinfection triggering epidemics where the threshold decreases with N) is expected whenever $1/\beta \ll \tau^{\text{inf,SIRS}} \ll \tau^{\text{rec,SIRS}}$, which corresponds to $b(\lambda) < \frac{\alpha}{\beta(\gamma-3)} \ln \kappa$ or, equivalently,

$$\lambda > \beta\vartheta(\alpha, \gamma) \equiv \beta / \left[\kappa^{\alpha/[\beta(\gamma-1)]} - 1 \right]. \quad (21)$$

Unless α is sufficiently small and/or γ is sufficiently large, this inequality is violated, and the hub lifetime is smaller than the hub infection time. This indicates that the hub activation scenario is not viable, and in analogy with the contact process, it hits towards a finite threshold. However, for sufficiently small $\vartheta(\alpha, \gamma)$, we can observe a region of λ values for which the hub activation mechanism is at work, leading to an effective threshold decreasing with N . A sufficient condition to observe this effective SIS-like behavior is $\beta\vartheta(\alpha, \gamma) < \lambda_c^{\text{SIS}}(N)$, the effective SIS threshold in the network of size N [12, 14, 32], since if the SIS dynamics cannot activate hubs in a network, SIRS dynamics cannot either, due to the suppressing effect of immunity. Assuming a scaling $\lambda_c^{\text{SIS}}(N) \sim k_{\text{max}}^{-\mu}$ where $\mu = 1/2$ for the QMF theory [11], this SIS-like behavior should be observed for network sizes $N \ll N_c \equiv [\beta\vartheta(\alpha, \gamma)]^{(\gamma-2)/\mu}$, crossing over to a constant threshold for $N \gg N_c$.

Numeric thresholds for $\gamma > 3$ are shown in Fig. 4. As we can see, for sufficiently small α (up to 1 for $\gamma = 4$), we

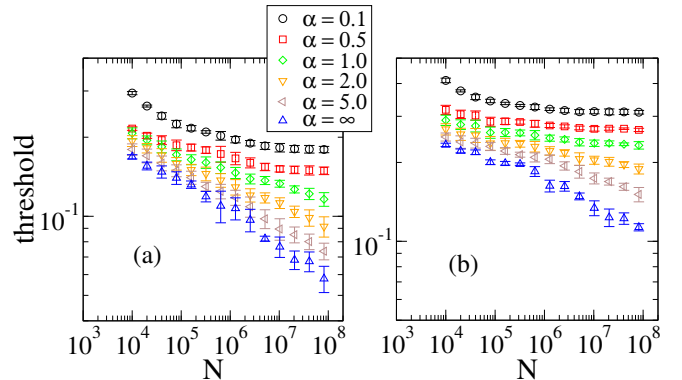


Figure 4. (color online) Epidemic threshold for SIRS model against network size for UCM networks with distinct degree exponents (a) $\gamma = 3.5$ and (b) $\gamma = 4.0$ with minimal degree $k_0 = 3$. This SIS limit ($\alpha = \infty$) is also included for comparison.

can observe a constant threshold for large N . For larger α values, the trend is still decreasing, being the constant plateau located on system sizes larger than those available to our computer resources.

IV. SIRS MODELS ON REAL NETWORKS

These results presented so far have been mainly checked on synthetic uncorrelated networks. They can however be extended to real correlated networks, characterized by conditional probability $P(k'|k)$ with a non-trivial dependence on k [28]. Focusing on the SIRS model, in Figures 5(a) and 5(b) we present numerical simulations on two SF real networks. We consider in particular the location-based social network Gowalla [33] and the product co-purchasing network in Amazon website [34], possessing degree exponents smaller and larger than 3, respectively, Figure 5(c). According QMF theory, the thresholds for these networks are equal to the inverse of the largest eigenvalue of their adjacency matrix. By means of a numerical diagonalization, we obtain the values $\lambda_c^{\text{QMF,Gowalla}} = 0.0059$ and $\lambda_c^{\text{QMF,Amazon}} = 0.042$. Our simulations show, in the case of the Gowalla network, with a degree exponent $\gamma \simeq 2.4 < 3$, that numerically estimated thresholds are essentially independent of α and very close to the QMF prediction. This behavior is consistent with the theoretical expectation of a hub activated dynamics, to be observed in the regime $\gamma < 3$, see Fig. 5(a). On the other hand, for the Amazon network, with degree exponent $\gamma \simeq 3.5 > 3$, we observe effective thresholds that diminish with increasing α , approaching the QMF prediction for $\alpha \rightarrow \infty$. This behavior is again in agreement with the prediction for the SIRS model in SF networks with $\gamma > 3$, that indicates a finite threshold for small α values, opposite to the QMF prediction of threshold independence.

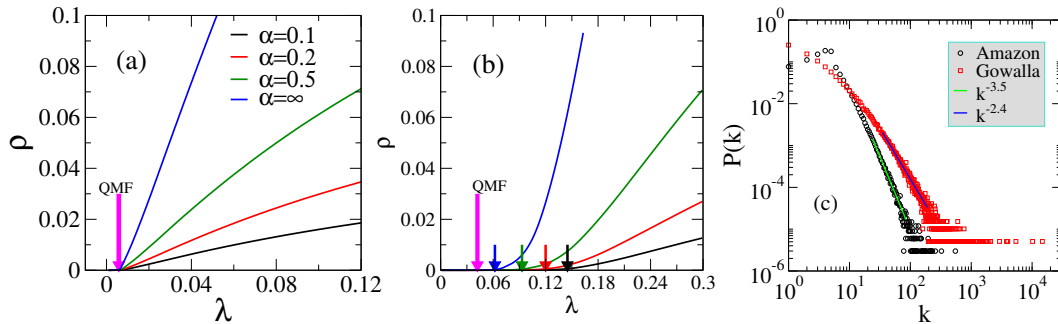


Figure 5. (Color online) Simulation of SIS and SIRS dynamics on real networks. Quasistationary density against infection rate in (a) Gowalla and (b) Amazon networks for different waning immunity rates. Arrows indicate the positions of the thresholds obtained via susceptibility method and QMF theory, see Appendix B. (c) Degree distribution for Gowalla ($N = 196591$, $k_{\max} = 14730$, $\gamma = 2.4$) and Amazon networks ($N = 334863$, $k_{\max} = 549$, $\gamma = 3.5$). Solid lines are power-law regressions.

V. SUMMARY

The determination of the properties of the epidemic transition in models of disease propagation in highly heterogeneous networks is a crucial topic in network science, to which a large research effort has been recently devoted. Among others, one of the main questions that remain to be answered in this field is what are the conditions under which a given epidemic model leads to a vanishing or a finite threshold, and how the properties of the epidemic transition can be best described from a theoretical point of view.

In the present paper, building on an extension of the theory of Ref. [14], we have proposed a general criterion to discern the nature of thresholds in epidemic models. The criterion is based in the comparison time scales of hub recovery (lifespan) and hub reinfection. When the lifespan is larger than the infection time, dynamics is triggered by a hub activation process, akin to the SIS dynamics: Hubs survive for very long times, and are able to reinfect each other, in such a way as to establish a long-lived endemic state. This hub activation scenario leads to a vanishing threshold when the lifespan is diverging in the thermodynamic limit. In this case, QMF theories are expected to be qualitatively correct. The reason underlying the effectiveness of QMF theories lies in the fact that they take into account the full topological structure of the network, and are dominated by the effects of the largest hubs. On the other hand, for a lifespan smaller than the infection time scale, hub activation cannot be sustained and possible epidemic phase transitions should be the result of a collective activation process, leading to a standard phase transition at a finite threshold, as in the case of the CP. In this second scenario, HMF theories should be qualitatively correct, due to the fact they work on the annealed network approximation, in which every node can interact with every other with a degree dependent probability [35].

To check the validity of the criterion, we have investigated a generic epidemic model with spontaneous recovering, waning immunity, and edge degree dependent

infection rates on scale-free networks, for which we can compute analytic expressions for the hub recovery and infection time scales. The model has as particular cases the fundamental epidemic models, as the SIS, SIRS and contact processes (CP) as well as more complex ones as the generalized SIS model of Ref. [23], which we have considered. After exemplifying our framework with the known cases of the SIS and CP models, we present an extended discussion of the SIRS model, an extension of the SIS model with waning immunity. While previous analytic approaches (HMF and QMF theories) predict for the SIRS model the same behavior than the SIS model, the main result from our criterion is that we are able to show that, instead, the effect of even a small amount of waning immunity is able to restore a finite threshold (albeit affected by possible strong finite-size effects) in scale-free networks with degree exponent $\gamma > 3$, at odds with the QMF theory valid for SIS in this regime, and in agreement with HMF. Our predictions are corroborated by means of numerical simulation on synthetic uncorrelated scale-free networks, as well as on real correlated networks.

The proposed criterion represents a step forward in our understanding of the properties of the epidemic transition in epidemic modeling, and thus opens the path to study more general and realistic models. In this sense, its application to more complex models is straightforward, only possible hampered by technical difficulties in extracting analytic expressions for the hub lifetime and infection time scales. These time scales can, however, be numerically estimated from direct simulations of epidemics on star networks, as we have shown in the examples presented here.

ACKNOWLEDGMENTS

This work was partially supported by the Brazilian agencies CAPES, CNPq, and FAPEMIG. R.P.-S. acknowledges financial support from the Spanish MINECO, under Project No. FIS2013-47282-C2-2, and ICREA Academia, funded by the Generalitat de Catalunya. R.P.-S is special

visiting researcher in the program *Ciência sem Fronteiras* - CAPES under project No. 88881.030375/2013-01.

Appendix A: Mean field theory of the KJI model on networks

In the Karsai, Juhász and Iglói (KJI) model [23], an edge transmits the infection from a vertex j to vertex i at a weighted rate $\lambda_{ij} = \lambda A_{ij}/(k_i k_j)^\theta$, where θ is a control parameter¹. The HMF theory for the KJI model is set in terms of the probability I_k that a node of degree k is infected, while it is susceptible with probability $1 - I_k$. The rate equation for this quantity can be simply written as [23, 35, 36]

$$\frac{dI_k}{dt} = -I_k + k(1 - I_k) \sum_{k'} \frac{\lambda}{(kk')^\theta} I_{k'} P(k'|k), \quad (\text{A1})$$

where $P(k'|k)$ is the probability that an edge from a node of degree k points to a node of degree k' [24]. The threshold is obtained by linearizing Eq. (A1) around the fixed point $I_k = 0$, which yields for uncorrelated networks with $P(k'|k) = k'P(k')/\langle k \rangle$ [28]

$$\frac{dI_k}{dt} = \sum_{k'} L_{kk'} I_{k'}, \quad (\text{A2})$$

with a Jacobian

$$L_{kk'} = -\delta_{kk'} + \lambda(kk')^{1-\theta} P(k)/\langle k \rangle. \quad (\text{A3})$$

The absorbing state $I_k = 0$ loses stability when the largest eigenvalue of $L_{kk'}$ is null. We thus obtain a threshold for the active state with the form

$$\lambda_c^{\text{HMF}} = \frac{\langle k \rangle}{\langle k^2(1-\theta) \rangle}. \quad (\text{A4})$$

As we see from this equation, $\theta = 0$ leads to the epidemic threshold of the SIS model, depending on γ , while $\theta = 1/2$ leads to the threshold of the CP model, independent of the network structure. For general values of θ , a finite HMF threshold is expected for $\gamma > 3 - 2\theta$, while it is null for $\gamma < 3 - 2\theta$.

From the point of view of QMF theory, based on the microscopic probability I_i that node i is infected, the relevant rate equation can be written as [2]

$$\frac{dI_i}{dt} = -I_i + \lambda(1 - I_i) \sum_j I_j \frac{A_{ij}}{(k_i k_j)^\theta}, \quad (\text{A5})$$

where A_{ij} is the adjacency matrix [2] with value $A_{ij} = 1$ if nodes i and j are connected, and zero otherwise, and we consider the normalization condition $I_i + S_i = 1$.

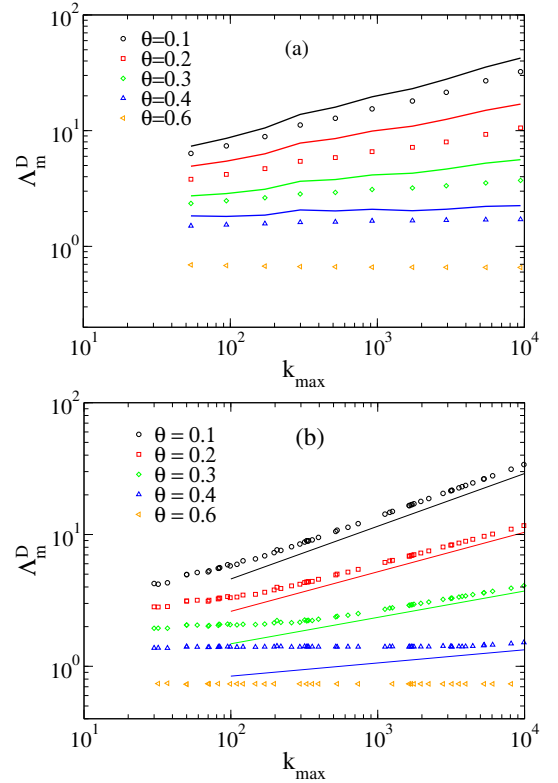


Figure 6. (color online) Scatter plot of the largest eigenvalue Λ_m^D of the matrix $D_{ij} = A_{ij}/(k_i k_j)^\theta$ against the degree of the most connected vertex k_{\max} for UCM networks with exponents (a) $\gamma = 2.7$ and (b) $\gamma = 3.5$ using minimal degree $k_0 = 3$ and structural cutoff $k_c \sim N^{1/2}$ [29]. The results were computed for 5 independent networks for $\gamma = 3.5$ and 1 for $\gamma = 2.7$ (largest degree fluctuates little). Sizes from $N = 10^3$, 3×10^3 , 10^4 , 3×10^4 , 10^5 , 3×10^5 , 10^6 , 3×10^6 , 10^7 , 3×10^7 , and 10^8 were used. In the bottom panel, solid lines are power laws $k_{\max}^{\frac{1}{2}-\theta}$. In the top panel, solid lines are proportional to $\Lambda_m/k_{\max}^\theta$, with Λ_m being the numerically estimated largest eigenvalue of the adjacency matrix A_{ij} for $\theta > 1/2$, and a constant for $\theta > 1/2$.

After linearization, stability analysis leads to a threshold inversely proportional to the largest eigenvalue Λ_m^D of the matrix

$$D_{ij} = \frac{A_{ij}}{(k_i k_j)^\theta}. \quad (\text{A6})$$

No general analytical expression is available for the largest eigenvalue of this matrix, so we have proceeded to determine it numerically in SF networks generated using the uncorrelated configuration model (UCM) [29], see Fig. 6. We find that $\Lambda_m^D \sim \Lambda_m/k_{\max}^\theta$ for $\theta < 1/2$, where Λ_m is the largest eigenvalue of the adjacency matrix A_{ij} for $\theta > 1/2$, and a constant for $\theta > 1/2$. For $\gamma > 3$, since $\Lambda_m \sim \sqrt{k_{\max}}$ [18], we have $\Lambda_m^D \sim k_{\max}^{\frac{1}{2}-\theta}$ for $\theta < 1/2$ and $\Lambda_m^D \sim \text{const.}$ for $\theta \geq 1/2$. The behavior of the largest eigenvalue in this case has strong finite size effects close to $\theta = 1/2$. These size effects can be observed in the

¹ A constant factor in the original definition was absorbed in λ .

crossover from a flat region to the scaling regime $k_{max}^{\frac{1}{2}-\theta}$ for $\theta < 1/2$, crossover that takes place at larger values of k_{max} when θ approaches $1/2$.

These observations indicate that, for $\theta < 1/2$, a zero threshold is obtained in the thermodynamic limit, independently of γ , while a finite threshold should occur for $\theta > 1/2$.

Appendix B: Mean field theories for the SIRS model on networks

In the HMF theory, the densities of infected, recovered and susceptible vertices of degree k , are represented by I_k , R_k , and S_k , respectively, and obey the normalization condition $I_k + R_k + S_k = 1$. The HMF dynamic equations, setting $\beta = 1$, are given by [22, 35, 36]

$$\frac{dI_k}{dt} = -I_k + \lambda k S_k \sum_{k'} I_{k'} P(k'|k), \quad (B1)$$

and

$$\frac{dR_k}{dt} = -\alpha R_k + I_k. \quad (B2)$$

To determine the threshold where an active state becomes stable, we perform a linear stability analysis around the fixed point $I_k = R_k = 0$, corresponding to the absorbing state. Since we are interested in long times, a quasi-static approximation [37] $\frac{dR_k}{dt} \approx 0$ is used to obtain $I_k = \alpha R_k$, which is inserted in Eq. (B1) to result in a linearized equation with Jacobian

$$L_{kk'} = -\delta_{kk'} + \lambda k P(k'|k). \quad (B3)$$

The absorbing state loses stability when the largest eigenvalue of $L_{kk'}$ is null. Thus, for uncorrelated networks with $P(k'|k) = k' P(k')/\langle k \rangle$, we easily obtain that the infected state is stable for [22]

$$\lambda > \lambda_c^{\text{HMF}} = \frac{\langle k \rangle}{\langle k^2 \rangle}. \quad (B4)$$

In the QMF theory, the process is defined in terms of the probabilities that a vertex i is infected, I_i , recovered, R_i , or susceptible, S_i , which fulfill the equations

$$\frac{dI_i}{dt} = -I_i + \lambda S_i \sum_j I_j A_{ij}, \quad (B5)$$

and

$$\frac{dR_i}{dt} = -\alpha R_i + I_i, \quad (B6)$$

where A_{ij} is the adjacency matrix [2], and we consider the normalization condition $I_i + R_i + S_i = 1$.

Applying a quasi-static approximation to Eqs. (B5) and (B6), we obtain the linearized equation

$$\frac{dI_i}{dt} = \sum_j L_{ij} I_j, \quad (B7)$$

with the Jacobian $L_{ij} = -\delta_{ij} + \lambda A_{ij}$, implying that the threshold is given by [38].

$$\lambda_c^{\text{QMF}} = \frac{1}{\Lambda_m}, \quad (B8)$$

where Λ_m is the largest eigenvalue of the adjacency matrix.

Appendix C: Simulation methods

SIRS simulations were implemented for $\beta = 1$ adapting the simulation scheme of Refs. [12, 32]: At each time step, the number of infected nodes N_i , the number of edges emanating from them N_k , and the number of recovered vertices N_r , are computed and time is incremented by $dt = 1/(N_i + \lambda N_k + \alpha N_r)$. With probability $N_i/(N_i + \lambda N_k + \alpha N_r)$ one infected node is selected at random and becomes recovered. With probability $\alpha N_r/(N_i + \lambda N_k + \alpha N_r)$, a recovered vertex is select and turned to susceptible. Finally, with probability $\lambda N_k/(N_i + \lambda N_k + \alpha N_r)$, an infection attempt is performed in two steps: (i) An infected vertex j is selected with probability proportional to its degree. (ii) A nearest neighbor of j is selected with equal chance and, if susceptible, is infected. If the chosen neighbor is infected or recovered nothing happens and simulation runs to the next time step. The numbers of infected and recovered nodes and links emanating from the former are updated accordingly, and the whole process is iterated.

KJI simulations were performed generalizing the previous algorithm as follows. For each node of the network we calculate the weight

$$w_i = \sum_j A_{ij} (k_i k_j)^{-\theta}, \quad (C1)$$

proportional to the total infection rate transmitted by all edges of i . Then, at each time step, the number of infected nodes N_i and the sum of the weights w_i over all infected nodes S_w are computed and time is incremented by $dt = 1/(N_i + \lambda S_w)$. With probability $N_i/(N_i + \lambda S_w)$ one infected node is selected at random and becomes susceptible. With probability $\lambda S_w/(N_i + \lambda S_w)$, an infection attempt is performed in two steps: (i) An infected vertex i is selected with probability proportional to its weight w_i . (ii) A nearest neighbor of i , namely j , is selected with probability proportional to $k_j^{-\theta}$ and, if susceptible, it is infected.

The simulations were performed using the quasi-stationary (QS) method [31, 39] which permits to overcome the difficulties intrinsic to the simulations of finite systems with absorbing states. In the QS method, every time the system visits an absorbing state it jumps to an active configuration previously visited during the simulation. This task is achieved building and constantly updating a list containing $M = 70$ configurations. The update is done by randomly picking up a stored configuration and

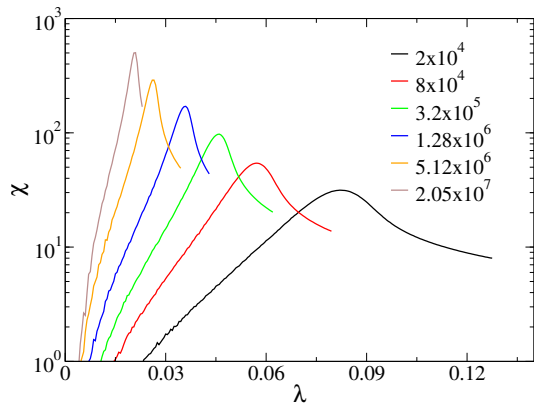


Figure 7. Susceptibility against infection rate for SIRS dynamics with $\alpha = 1.0$. We used UCM networks of different sizes (quoted in the labels) with $k_0 = 3$ and $\gamma = 2.7$.

replacing it by the current one with probability $p_r \Delta t$. We fixed $p_r \simeq 10^{-2}$ since no dependence on this parameters was detected for a wide range of simulation parameters. After a relaxation time t_r , averages are computed over a time t_{av} . Typically, a QS state is reached at times $t \gtrsim 10^4$ for QS simulations of dynamical processes on complex networks. Therefore, $t_r = 10^5$ was used in all simulation.

On the other hand, averaging times from 10^6 to 10^8 were used, the larger the average time the smaller the infection rate.

During the averaging time, the QS probability $\bar{P}(n)$ that the system has n infected vertices is computed. All stationary quantities of interest can be derived from $\bar{P}(n)$. Here, we will investigate the density of infected vertices $\rho = \sum_n n \bar{P}(n) / N$, the lifespan $\tau = 1 / \bar{P}(1)$ and the susceptibility defined as $\chi = N(\langle \rho^2 \rangle - \langle \rho \rangle^2) / \langle \rho \rangle$ [12]. This susceptibility has a diverging peak at the transition to an absorbing state on complex networks [12, 21, 40] and has been successfully used to determine the thresholds for epidemic models [12, 38, 41, 42].

Simulations were done on SF networks with N vertices and degree distribution $P(k) \sim k^{-\gamma}$ generated with the uncorrelated configuration model (UCM) [29] with minimum degree $k_0 = 3$ and structural upper cutoff $k_{max} = N^{1/2}$, which guarantees absence of degree correlations in the networks generated, that are, therefore, suitable for comparisons with the HMF theory where this simplification was adopted. Averages were computed using more than 20 different network samples.

The determination of the threshold, estimated as the peak of susceptibility, is shown in Fig. 7.

-
- [1] R. Pastor-Satorras, C. Castellano, P. Van Mieghem, and A. Vespignani, *Rev. Mod. Phys.* **87**, 925 (2015).
- [2] M. Newman, *Networks: An Introduction* (Oxford University Press, New York, NY, USA, 2010).
- [3] D. Easley and J. Kleinberg, *Networks, Crowds, and Markets: Reasoning About a Highly Connected World* (Cambridge University Press, New York, NY, USA, 2010).
- [4] C. Castellano, S. Fortunato, and V. Loreto, *Rev. Mod. Phys.* **81**, 591 (2009).
- [5] A.-L. Barabási and R. Albert, *Science* **286**, 509 (1999).
- [6] R. M. Anderson and R. M. May, *Infectious diseases in humans* (Oxford University Press, Oxford, 1992).
- [7] R. Pastor-Satorras and A. Vespignani, *Phys. Rev. Lett.* **86**, 3200 (2001).
- [8] M. Boguñá and R. Pastor-Satorras, *Phys. Rev. E* **66**, 047104 (2002).
- [9] D. Chakrabarti, Y. Wang, C. Wang, J. Leskovec, and C. Faloutsos, *ACM Trans. Inf. Syst. Secur.* **10**, 1 (2008).
- [10] S. Chatterjee and R. Durrett, *Ann. Probab.* **37**, 2332 (2009).
- [11] C. Castellano and R. Pastor-Satorras, *Phys. Rev. Lett.* **105**, 218701 (2010).
- [12] S. C. Ferreira, C. Castellano, and R. Pastor-Satorras, *Phys. Rev. E* **86**, 041125 (2012).
- [13] C. Castellano and R. Pastor-Satorras, *Scientific Reports* **2** (2012).
- [14] M. Boguñá, C. Castellano, and R. Pastor-Satorras, *Phys. Rev. Lett.* **111**, 068701 (2013).
- [15] T. Mountford, J.-C. Mourrat, D. Valesin, and Q. Yao, *arXiv:1203.2972v1* (2013).
- [16] A. V. Goltsev, S. N. Dorogovtsev, J. G. Oliveira, and J. F. F. Mendes, *Phys. Rev. Lett.* **109**, 128702 (2012).
- [17] R. Pastor-Satorras and A. Vespignani, *Phys. Rev. E* **63**, 066117 (2001).
- [18] F. Chung, L. Lu, and V. Vu, *Proc. Natl. Acad. Sci. USA* **100**, 6313 (2003).
- [19] C. Castellano and R. Pastor-Satorras, *Phys. Rev. Lett.* **96**, 038701 (2006).
- [20] S. C. Ferreira, R. S. Ferreira, C. Castellano, and R. Pastor-Satorras, *Phys. Rev. E* **84**, 066102 (2011).
- [21] A. S. Mata, R. S. Ferreira, and S. C. Ferreira, *New J. Phys.* **16**, 053006 (2014).
- [22] J.-D. Bancal and R. Pastor-Satorras, *Eur. Phys. J. B* **76**, 109 (2010).
- [23] M. Karsai, R. Juhász, and F. Iglói, *Phys. Rev. E* **73**, 036116 (2006).
- [24] R. Pastor-Satorras, A. Vázquez, and A. Vespignani, *Phys. Rev. Lett.* **87**, 258701 (2001).
- [25] M. Abramowitz and I. A. Stegun, *Handbook of mathematical functions*. (Dover, New York, 1972).
- [26] J. A. Hołyst, J. Sienkiewicz, A. Fronczak, P. Fronczak, and K. Suchecki, *Phys. Rev. E* **72**, 026108 (2005).
- [27] M. Boguñá, R. Pastor-Satorras, and A. Vespignani, *Eur. Phys. J. B* **38**, 205 (2004).
- [28] S. N. Dorogovtsev and J. F. F. Mendes, *Advances in Physics* **51**, 1079 (2002).
- [29] M. Catanzaro, M. Boguñá, and R. Pastor-Satorras, *Phys. Rev. E* **71**, 027103 (2005).
- [30] S. Gúmez, A. Arenas, J. Borge-Holthoefer, S. Meloni, and Y. Moreno, *Eur. Lett.* **89**, 38009 (2010).
- [31] M. M. de Oliveira and R. Dickman, *Phys. Rev. E* **71**, 016129 (2005).

- [32] A. S. Mata and S. C. Ferreira, *Phys. Rev. E* **91**, 012816 (2015).
- [33] E. Cho, S. A. Myers, and J. Leskovec, in *Proceedings of the 17th ACM SIGKDD International Conference on Knowledge Discovery and Data Mining*, KDD '11 (ACM, New York, NY, USA, 2011) pp. 1082–1090.
- [34] J. Yang and J. Leskovec, *Knowledge and Information Systems* **42**, 181 (2015).
- [35] S. N. Dorogovtsev, A. V. Goltsev, and J. F. F. Mendes, *Rev. Mod. Phys.* **80**, 1275 (2008).
- [36] A. Barrat, M. Barthélemy, and A. Vespignani, *Dynamical Processes on Complex Networks* (Cambridge University Press, Cambridge, 2008).
- [37] M. Catanzaro, M. Boguñá, and R. Pastor-Satorras, *Phys. Rev. E* **71**, 056104 (2005).
- [38] A. S. Mata and S. C. Ferreira, *Eur. Lett.* **103**, 48003 (2013).
- [39] S. C. Ferreira, R. S. Ferreira, and R. Pastor-Satorras, *Phys. Rev. E* **83**, 066113 (2011).
- [40] R. S. Ferreira and S. C. Ferreira, *Eur. Phys. J. B* **86**, 1 (2013).
- [41] H. K. Lee, P.-S. Shim, and J. D. Noh, *Phys. Rev. E* **87**, 062812 (2013).
- [42] W. Wang, M. Tang, H. Yang, Y. Do, Y.-C. Lai, and G. Lee, *Scientific reports* **4** (2014).